$$\text{(TPP)Fe}^{\text{III}}\text{–O–Fe}^{\text{IV}}(\text{TPP}^{\bullet+})(\text{O}) + \text{CH}_2\text{Cl}_2 \rightarrow \text{(TPP)Fe}^{\text{III}}\text{–O–Fe}^{\text{IV}}(\text{TPP})(\text{OH}) + {}^{\bullet}\text{CHCl}_2 \tag{7a}$$

$$\text{(TPP)Fe}^{\text{III}}\text{–O–Fe}^{\text{IV}}(\text{TPP})(\text{OH}) + {}^{\bullet}\text{CHCl}_2 \rightarrow ((\text{TPP})\text{Fe}^{\text{III}})_2\text{O} + \text{HC(O)Cl} + \text{HCl} \tag{7b}$$

$$\text{(TPP)Fe}^{\text{III}}\text{–O–Fe}^{\text{IV}}(\text{TPP}^{\bullet+})(\text{O}) + \text{HC(O)Cl} \rightarrow ((\text{TPP})\text{Fe}^{\text{III}})_2\text{O} + \text{CO}_2 + \text{HCl} \tag{7c}$$

$$((\text{TPP})\text{Fe}^{\text{III}})_2\text{O} + \text{HCl} \rightarrow (\text{TPP})\text{Fe}^{\text{III}}\text{OH} + (\text{TPP})\text{Fe}^{\text{III}}(\text{Cl}) \tag{7d}$$

accompanies solvent oxidation and the formation of Cl^- ions. Carbon dioxide has been identified as an oxidation product of CH_2Cl_2 in the reaction of $\text{C}_6\text{H}_5\text{IO}$ with Ni(II) macrocycles in CH_2Cl_2.[18] Monomerization of $((\text{TPP})\text{Fe}^{\text{III}})_2\text{O}$ may also occur on its reaction with DAO (eq 8). It has been observed that the

$$((\text{TPP})\text{Fe}^{\text{III}})_2\text{O} + \text{DAO} \rightarrow (\text{TPP})\text{Fe}^{\text{III}}\text{–O–Fe}^{\text{III}}(\text{DAO})(\text{TPP}) \tag{8a}$$

$$(\text{TPP})\text{Fe}^{\text{III}}\text{–O–Fe}^{\text{III}}(\text{DAO})(\text{TPP}) \rightarrow (\text{TPP})\text{Fe}^{\text{III}}(\text{O}^-) + (\text{TPP})\text{Fe}^{\text{III}}(\text{DAO}) \tag{8b}$$

$$(\text{TPP})\text{Fe}^{\text{III}}(\text{DAO}) + \text{DAO} \rightarrow (\text{TPP})\text{Fe}^{\text{III}}(\text{DAO})_2^- \tag{8c}$$

addition of a large excess of PO to $((\text{TPP})\text{Fe}^{\text{III}})_2\text{O}$ results in the appearance of the characteristic spectrum[14] of $(\text{TPP})\text{Fe}^{\text{III}}(\text{PO})_2^-$.

Addition of TME to the reaction mixture of $((\text{TPP})\text{Fe}^{\text{III}})_2\text{O}$ and DAO provides TME-epoxide as the product along with other oxidized amine products. The second-order rate constants determined from the initial rates remain reasonably constant at various concentrations of TME (0.01–1.0 M), showing that TME epoxidation is not rate-limiting. As expected, the distribution of the various products changes with respect to $[\text{TME}]_i$ (Table I) since DA etc. compete with TME for oxidation. When the concentration of TME is increased to 1.0 M, the yields of DA and TME-epoxide reach 94% and $((\text{TPP})\text{Fe}^{\text{III}})_2\text{O}$ remains, spectrally, intact during the course of the reaction. This establishes that when there is a large excess of TME, the hypervalent iron–oxo porphyrin species is trapped totally to provide 100% yields of DA and TME-epoxide and that under such a condition solvent is not oxidized and there is no formation of $(\text{TPP})\text{Fe}^{\text{III}}(\text{Cl})$.

The epoxidizing species could be $({}^{+\bullet}\text{TPP})\text{Fe}^{\text{IV}}(\text{O})\text{–O–Fe}^{\text{III}}(\text{TPP})$ (eq 9), $(\text{TPP})\text{Fe}^{\text{IV}}(\text{O}^-)\text{–O–Fe}^{\text{IV}}(\text{TPP})$ (eq 10), or $({}^{+\bullet}\text{TPP})\text{Fe}^{\text{IV}}(\text{O})$ (eq 11). To account for the initial rates in the presence of high

$$((\text{TPP})\text{Fe}^{\text{III}})_2\text{O} + \text{DAO} \rightarrow ({}^{+\bullet}\text{TPP})\text{Fe}^{\text{IV}}(\text{O})\text{–O–Fe}^{\text{III}}(\text{TPP}) \tag{9}$$

$$({}^{+\bullet}\text{TPP})\text{Fe}^{\text{IV}}(\text{O})\text{–O–Fe}^{\text{III}}(\text{TPP}) \rightarrow (\text{TPP})\text{Fe}^{\text{IV}}(\text{O}^-)\text{–O–Fe}^{\text{IV}}(\text{TPP}) \tag{10}$$

$$({}^{+\bullet}\text{TPP})\text{Fe}^{\text{IV}}(\text{O})\text{–O–Fe}^{\text{III}}(\text{TPP}) \rightarrow (\text{TPP})\text{Fe}^{\text{III}}(\text{O}^-) + ({}^{+\bullet}\text{TPP})\text{Fe}^{\text{IV}}(\text{O}) \tag{11}$$

$[\text{TME}]_i$ the initial epoxidant trapped by TME must be $({}^{+\bullet}\text{TPP})\text{Fe}^{\text{IV}}(\text{O})\text{–O–Fe}^{\text{III}}(\text{TPP})$. After the initial lag phase the epoxidant is reasonably $({}^{+\bullet}\text{TPP})\text{Fe}^{\text{IV}}(\text{O})$, which after oxygen transfer to substrate is complete, reconverts to the $((\text{TPP})\text{Fe}^{\text{III}})_2\text{O}$ state. The $(\text{TPP})\text{Fe}^{\text{IV}}(\text{O}^-)\text{–O–Fe}^{\text{IV}}(\text{TPP})$ species is likely to be unimportant as an epoxidant. Thus, at low temperatures iron(IV)–oxo porphyrin shows no reactivity with alkenes.[19]

Acknowledgment. This work was supported by the National Institutes of Health.

Registry No. DAO, 62820-00-2; TME, 563-79-1; $((\text{TPP})\text{Fe}^{\text{III}})_2\text{O}$, 12582-61-5.

---

[18] Koola, J. D.; Kochi, J. K. *Inorg. Chem.* **1987**, *26*, 916.

[19] (a) Mansuy, D. *Pure Appl. Chem.* **1987**, *59*, 759. (b) Balch, A. L., private communication.

Contribution from the Department of Chemistry,
University of Colorado at Colorado Springs,
Colorado Springs, Colorado 80933-7150

Synthesis, Characterization, and Solvatochromic Studies of Group 6 Metal Carbonyls Bound to the Bridging Ligand 2,3-Bis(2-pyridyl)pyrazine (dpp)

M. Shoup, B. Hall, and R. R. Ruminski*

Received June 29, 1987

Recent investigations have used the bidentate nitrogen aromatic heterocyclic ligands 2,3-bis(2-pyridyl)pyrazine (dpp),[1,2] 2,2′-bipyrimidine (bpym),[3-5] and 2,3-bis(2-pyridyl)quinoxaline (dpq)[6] in the preparation of mono- and bimetallic Ru(II) polyazine complexes. Interest in Ru(L)_3^{2+} (L = bpy, bpym, dpp, or dpq) arises from the fact that these complexes possess highly absorbing MLCT transitions in the visible spectrum, are photoinert, and undergo emission in fluid solution with lifetimes of several hundreds of nanoseconds.[1,2,4,6-8] These photophysical properties make such complexes ideal in bimolecular photocatalyzed water-splitting or energy-transfer processes.[8-15] Polymetallic intramolecular energy transfer has been explored as an alternative approach that bypasses the considerable difficulties associated with bimolecular energy transfer.[2] The polymetallic complex incorporates a highly absorbing, photoinert antenna fragment that can transfer energy through a bridging ligand, such as dpp or bpym, to a remote reactive metal fragment that does not absorb visible radiation.

Cr, Mo, and W carbonyl fragments bound to nitrogen aromatic bridging ligands have received some attention as antenna fragments in these polymetallic complexes.[16] An advantage of metal carbonyl antenna fragments is the negative solvatochromism of the MLCT transition in a wide variety of solvents.[16-22] With use of only differential solvents, the energy of the MLCT state of the antenna fragment could potentially be tuned to probe or exploit the acceptor levels of the reactive fragment.

Our research group has been involved in the preparation and characterization of potential antenna complexes containing the bridging ligands bpym or dpp.[23] We wish to report the prepa-

---

[1] Braunstein, C. H.; Baker, A. D.; Strekas, T. C.; Gafney, H. D. *Inorg. Chem.* **1984**, *23*, 857.

[2] Brewer, K. J.; Murphy, R. W., Jr.; Spurlin, S. R.; Petersen, J. D. *Inorg. Chem.* **1986**, *25*, 883.

[3] Dose, E. V.; Wilson, L. J. *Inorg. Chem.* **1978**, *17*, 2660.

[4] Hunziker, M.; Ludi, A. *J. Am. Chem. Soc.* **1977**, *99*, 7370.

[5] Ruminski, R. R.; Petersen, J. D. *Inorg. Chem.* **1982**, *21*, 3706.

[6] Rillema, D. P.; Taghdiri, D. G.; Jones, D. S.; Keller, C. D.; Worl, L. A.; Meyer, T. J.; Levy, H. A. *Inorg. Chem.* **1987**, *26*, 578.

[7] Navon, G.; sutin, N. *Inorg. Chem.* **1974**, *13*, 2159.

[8] Lin, C.-T.; Sutin, N. *J. Phys. Chem.* **1976**, *80*, 97.

[9] Balzani, V.; Moggi, L.; Manfrin, M. F.; Bolletta, F.; Laurence, G. A. *Coord. Chem. Rev.* **1975**, *15*, 321.

[10] Lin, C.-T.; Bottcher, W.; Chou, M.; Creutz, C.; Sutin, N. *J. Am. Chem. Soc.* **1976**, *98*, 6536.

[11] Kavarnos, G. J.; Turro, N. J. *Chem. Rev.* **1986**, *86*, 401.

[12] Dressick, W. J.; Meyer, T. J.; Durham, B.; Rillema, D. P. *Inorg. Chem.* **1982**, *21*, 3451.

[13] Bock, C. R.; Conner, J. A.; Gutierrez, A. R.; Meyer, T. J.; Whitten, D. G.; Sullivan, B. P.; Nagle, J. K. *J. Am. Chem. Soc.* **1979**, *101*, 4815.

[14] De Laive, P. J.; Sullivan, B. P.; Meyer, T. J.; Whitten, D. G. *J. Am. Chem. Soc.* **1979**, *101*, 4007.

[15] Rillema, D. P.; Allen, G.; Meyer, T. J.; Conrad, D. *Inorg. Chem.* **1983**, *22*, 1617.

[16] Moore, K. J.; Petersen, J. D. *Polyhedron* **1983**, *2*, 279.

[17] Lever, A. B. P. *Inorganic Electronic Spectroscopy*, 2nd ed.; Elsevier: Amsterdam, 1984.

[18] Kaim, W.; Kohlmann, S. *Inorg. Chem.* **1986**, *25*, 3306.

[19] Ernst, S.; Kaim, W. *J. Am. Chem. Soc.* **1986**, *108*, 3578.

[20] Ernst, S.; Kurth, Y.; Kaim, W. *J. Organomet. Chem.* **1986**, *302*, 211.

[21] Manuta, D. M.; Lees, A. J. *Inorg. Chem.* **1983**, *22*, 3825.

[22] Overton, C.; Conner, J. A. *Polyhedron* **1982**, *1*, 53.

[23] (a) Ruminski, R.; Johnson, J. *Inorg. Chem.* **1987**, *26*, 210. (b) Ruminski, R.; Wallace, I. *Polyhedron* **1987**, *6*(8), 1673. (c) Hiskey, M. A.; Ruminski, R. *Inorg. Chim. Acta* **1986**, *112*, 189. (d) Ruminski, R.; Van Tassel, K. D.; Petersen, J. D. *Inorg. Chem.* **1984**, *23*, 4380. (e) Ruminski, R.; Petersen, J. D. *Inorg. Chim. Acta* **1985**, *97*, 129. (f) Ruminski, R. *Inorg. Chim. Acta* **1985**, *103*, 159.

0020-1669/88/1327-0200$01.50/0

ration, solvatochromic UV–visible electronic absorption spectra, ^{13}C NMR spectra, and electrochemistry of some monometallic and homo- and heterobimetallic (M = Cr, Mo, and W) carbonyl complexes bound to/through the bridging ligand dpp.

Experimental Section

Materials. $M(CO)_6$ (M = Cr, Mo, and W), 2,3-bis(2-pyridyl)pyrazine (dpp), and CD_2Cl_2 were obtained from Aldrich Chemicals and used without modification. All other chemicals were AR grade. Elemental analyses were performed by Atlantic Microlab, Atlanta, GA.

Instrumentation. Electronic absorption spectra (accuracy ±3 nm) were recorded on a Beckman Model 5240 spectrophotometer with matching quartz cells.

Cyclic voltammograms were recorded on a Bio Analytic Systems CV-1B cyclic voltammograph with a Hewlett-Packard 7044A XY recorder. A Ag/AgCl (3 M KCl, nominally −0.044 V vs SCE) reference electrode and glassy-carbon working electrode were used. All potentials are reported vs Ag/AgCl and are uncorrected for junction potentials. The potentials reported for oxidation couples, $E_{1/2}$, were estimates obtained by averaging anodic and cathodic peak potentials, unless otherwise noted.

Proton-decoupled ^{13}C NMR spectra were obtained on a Bruker Model WM-250 Fourier transform NMR spectrometer operating at 62.9 MHz. Samples were run in a 10.0-mm probe with 30% deuteriated dichloromethane as an internal lock and reference (δ = 53.8).

Infrared spectra were recorded as solid KBr samples on a Nicolet Model 20DX FTIR instrument using a 1-cm^{-1} resolution.

Syntheses. $[W(CO)_4]_2$dpp. A mixture of 0.20 g (0.85 mmol) of dpp and 1.5 g (4.27 mmol) of $W(CO)_6$ in 50 mL of toluene was heated at reflux for 48 h under Ar in the dark. After the mixture was cooled to room temperature, 100 mL of petroleum ether was added and the solution was capped and refrigerated overnight. The precipitate was collected on a sintered-glass filter funnel by filtration. The product was redissolved on the funnel with a minimum amount of CH_2Cl_2 and suction-filtered to remove insoluble material. The liquid was loaded onto a 25 cm × 3 cm diameter alumina column, and the column was eluted with CH_2Cl_2. The blue bimetallic product was collected, rotary evaporated to dryness, and stored in the dark under vacuum at room temperature. The dissolution and chromatographic process was repeated three times to achieve satisfactory product purification; yield 0.34 g (0.41 mmol), 48%. Anal. Calcd for $C_{22}H_{10}N_4O_8W_2$: C, 31.99; H, 1.22; N, 6.78. Found: C, 32.38; H, 1.57; N, 6.63.

$[Cr(CO)_4]_2$dpp. A mixture of 0.30 g (1.28 mmol) of dpp and 1.40 g (6.36 mmol) of $Cr(CO)_6$ in 50 mL of toluene was heated at reflux for 24 h under Ar in the dark. The product was isolated and purified as described above for $[W(CO)_4]_2$dpp; yield 0.27 g (0.45 mmol), 34%. Anal. Calcd for $C_{22}H_{10}N_4O_8Cr_2\cdot{}^1/_2CH_2Cl_2$: C, 44.67; H, 1.84; N, 9.26. Found: C, 44.92; H, 1.98; N, 9.22. Additional drying (72 h) under vacuum at 35 °C produced product decompositon.

$[W(CO)_4]$dpp$[Mo(CO)_4]$. A mixture of 0.23 g (0.44 mmol) of $[W(CO)_4]$dpp and 0.14 g (0.53 mmol) of $Mo(CO)_6$ in 50 mL of toluene was heated at reflux for 22 h under Ar in the dark. After the mixture was cooled to room temperature, 100 mL of petroleum ether was added and the solution was capped and refrigerated overnight. The solid was collected on a sintered-glass filter funnel. The crude product was then dissolved on the funnel with 50 mL of CH_2Cl_2 and suction-filtered to remove insoluble material. After addition of 50 mL of petroleum ether to the solution, it was sealed and refrigerated overnight to reprecipitate the product. The solid was again collected on a filter funnel, and the purple wash (unreacted $[W(CO)_4]$dpp) was discarded. The reprecipitation process was repeated three times, at which time the wash was colorless; yield 0.25 g (0.34 mmol), 77%. Anal. Calcd for $C_{22}H_{10}N_4O_8WMo$: C, 35.80; H, 1.64; N, 7.59. Found: C, 35.60; H, 1.57; N, 7.49.

$[Cr(CO)_4]$dpp$[Mo(CO)_4]$. A mixture of 0.10 g (0.23 mmol) of $[Mo(CO)_4]$dpp and 0.25 g (1.14 mmol) of $Cr(CO)_6$ in 50 mL of toluene was heated at reflux for 5 h under Ar in the dark. After the mixture was cooled to room temperature, 100 mL of petroleum ether was added and the solution was sealed and refrigerated overnight. The solid was collected by filtration on a filter funnel. The product was dissolved in 25 mL of CH_2Cl_2 on the funnel and the solution suction-filtered to remove insoluble material. After addition of 60 mL of petroleum ether, the solution was sealed and refrigerated overnight to reprecipitate the product. The product was purified by reprecipitation three times as described above; yield 0.034 g (0.056 mmol), 24%. Anal. Calcd for $C_{22}H_{10}N_4O_8CrMo$: C, 43.58; H, 1.66; N, 9.24. Found: C, 43.44; H, 1.74; N, 9.22.

$[Cr(CO)_4]$dpp$[W(CO)_4]$. A mixture of 0.10 g (0.19 mmol) of $[W(CO)_4]$dpp and 0.22 g (1.00 mmol) of $Cr(CO)_6$ in 50 mL of toluene was heated at reflux for 5 h under Ar in the dark. The product was isolated and purified as described above for $[Cr(CO)_4]$dpp$[Mo(CO)_4]$; yield 0.0314 g (0.045 mmol), 24%. Anal. Calcd for $C_{22}H_{10}N_4O_8CrW\cdot{}^1/_2CH_2Cl_2$: C, 36.66; H, 1.73; N, 7.61. Found: C, 35.77; H, 1.64; N, 7.63.

Table I. Electronic Absorption Data for $[M(CO)_4]_{1,2}L$ Complexes in CH_2Cl_2

complex	λ_{max}, nm	$10^{-3}\epsilon$, M^{-1} cm^{-1}	assignt	ref
$[Cr(CO)_4]_2$dpp	645	13	MLCT	*a*
	385 (sh)[b]	6.7	LF	
	325	28	MLCT	
$[Mo(CO)_4]_2$dpp	610	12	MLCT	23a
	380 (sh)	6.0	LF	
	320 (sh)	19	MLCT	
	300	22	intraligand	
$[W(CO)_4]_2$dpp	635	19	MLCT	*a*
	390 (sh)	8.6	LF	
	330	23	MLCT	
	305	20	intraligand	
$[Mo(CO)_4]$dpp$[W(CO)_4]$	625	20	MLCT	*a*
	385 (sh)	8.6	LF	
	330	26	MLCT	
	305	27	intraligand	
$[Mo(CO)_4]$dpp$[Cr(CO)_4]$	625	16	MLCT	*a*
	380 (sh)	8.3	LF	
	325	30	MLCT	
	305	27	intraligand	
$[W(CO)_4]$dpp$[Cr(CO)_4]$	640	18	MLCT	*a*
	380 (sh)	7.8	LF	
	330	27	MLCT	
	305	23	intraligand	
$[Mo(CO)_4]$bpym	508		MLCT	16
	379		LF	
$[Mo(CO)_4]_2$bpym	675		MLCT	16
	440		MLCT	

[a] This work. [b] sh = shoulder.

$[M(CO)_4]$dpp. These complexes were prepared as previously reported.[23b]

Results and Discussion

The electronic absorption spectra of the hetero- and homobimetallic complexes were recorded in solvents of different polarity. The bimetallic octacarbonyl complexes exhibited intense (ϵ > 1000 M^{-1} cm^{-1}) solvent-dependent transitions in the visible spectrum (Table I). Due to the large molar absorptivity of the solvent-dependent lowest energy transition and by analogy to the spectra of previously reported metal carbonyl α-diimine complexes,[17-22,23a,b] the lowest energy absorptions of the $[M(CO)_4]$dpp$(M'(CO)_4]$ complexes are assigned as dpp $p_\pi^* \leftarrow$ M d_π transitions. All complexes also exhibited solvent-independent transitions between 370 and 390 nm, which based on solvent independence and analogy with previously reported complexes,[16,18,23a,b,24,25] are assigned as $^1A_1,{}^1E_1 \leftarrow {}^1A_1$ ligand field transitions.

The bimetallic dpp-bridged complexes displayed MLCT transitions at lower energy than the respective monometallic complexes.[23a] Similar results for other bimetallic complexes have been attributed to the formation of a M d_π–bridging ligand p_π^*–M d_π nonbonding molecular orbital and a lowering of the bridging ligand p_π^* LUMO in bimetallic complexes.[1,3,5,16,22] Hetero- and homobimetallic Cr, Mo, and W octacarbonyl complexes bound to/through the bpym bridging ligand exhibited wavelength increases of 150–200 nm vs the wavelengths of the monometallic complexes in CH_2Cl_2.[16,22] The identical dpp-bridged complexes underwent only a 100-nm increase in CH_2Cl_2. Previous comparisons of monometallic $[M(CO)_4]$dpp and $[M(CO)_4]$bpym complexes[23b] showed identical MLCT energies in CH_2Cl_2, indicating approximate parity of the electron-withdrawing ability and LUMO of dpp and bpym. Therefore, the smaller wavelength increase of dpp- vs that of bpym-bridged bimetallic complexes is probably due to less effective metal–metal interactions through

---

(24) Wrighton, M. S.; Morse, D. L. *J. Organomet. Chem.* **1975**, *97*, 405.
(25) Balk, R. W.; Snoeck, T.; Stufkens, D. J.; Oskam, A. *Inorg. Chem.* **1980**, *19*, 3015.

Table II. Infrared[a] and Electrochemical[b] Data for $[Mo(CO)_4]_{1,2}$dpp Complexes

	infrared freq ν_{CO}, cm^{-1}				
metal(s)	A_1	B_1	A_1	B_2	oxidn potentials
Cr	2008	1906	1889	1825	+0.56
Mo	2016	1914	1882	1819	+0.79[c]
W	2003	1902	1872	1824	+0.80[c]
Cr–Cr	2006	1915	1884	1834	+0.57
Mo–Mo	2012	1905	1879	1824	+0.80[c]
W–W	2003	1912	1868	1827	+0.79
Cr–Mo	2011	1916 (sh)	1890	1836	+0.58, +0.80
Cr–W	2005	1915	1882	1830	+0.58, +0.80
Mo–W	2008	1928	1882	1830	+0.80

[a] Infrared spectra recorded in KBr pellets. [b] Cyclic voltammetry in CH_2Cl_2, containing 0.1 M TBAP, at 100 mV/s vs Ag/AgCl electrode. Potential of the oxidation wave reported for the irreversible W and Mo complexes. [c] Remeasured values from ref 23a,b.

the dpp bridging ligand, rather than increased stabilization of the dpp $p_\pi{}^*$ LUMO.

Cyclic voltammograms of the Mo and W dpp-bridged complexes show irreversible oxidations with no return cathodic waves. The reported potentials (Table II) for Mo and W complexes are the observed oxidation waves, rather than average oxidation/reduction couples. Results show oxidation of the metal centers in bimetallic complexes occurred at the same potential as for the respective monometallic dpp complexes. Previously reported results for the bpym-bridged complexes showed oxidation potentials increased 0.15–0.18 V compared with those of the respective monometallic bpym complexes, which indicated substantial metal–metal interaction.[1,3,5] The absence of any electrochemical oxidation potential change in dpp-bridged bimetallic vs monometallic complexes may be interpreted as indicating little metal–metal interaction occurs through the dpp bridging ligand. The lack of substantial metal–metal interaction for dpp-bridged Ru(II) systems has previously been attributed to a nonplanar configuration of dpp due to 3′-H–3″-H steric repulsion.[1]

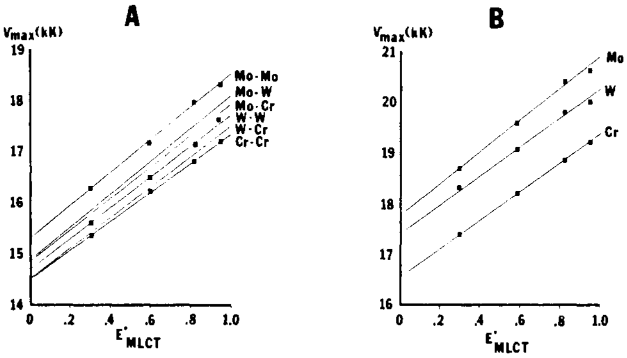

Figure 1. Plots of ν_{max}(MLCT) energies (10^3 cm^{-1}) vs E^*_{MLCT} for (A) $[M(CO)_4]dpp[M'(CO)_4]$ and (B) $[M(CO)_4]$dpp complexes. Data points for heterobimetallic complexes are omitted for clarity in (A).

The energy (10^3 cm^{-1}) of the lowest energy MLCT transition of the mono- and bimetallic dpp complexes was obtained from the absorption spectra of the complexes in toluene, THF, acetone, and DMF (Table III). The MLCT energy (ν_{max} (10^3 cm^{-1})) of a complex was plotted vs the E^*_{MLCT} solvent parameter for the solvent in which the spectrum was obtained (Figure 1). The solvent sensitivity has previously been defined as $B = \nu_{max}/E^*_{MLCT}$.[18,21]

The generally observed shift to higher energy of the MLCT transition in solvents of higher polarity has been attributed to ground-state stabilization of noncentrosymmetric complexes in more polar solvents.[17] Recent studies on centrosymmetric bimetallic complexes, such as $[Mo(CO)_4]_2$bpym, reported that these complexes were more solvent sensitive than their monometallic analogues.[18-20] Additional factors, including molecular polarizability and σ-donating and π-back-bonding ability of the ligand, have been utilized in the interpretation of the solvatochromic behavior.

Table III. MLCT Absorption Maxima ν_{max} of $[M(CO)_4]$dpp and $[M(CO)_4]dpp[M'(CO)_4]$ Complexes in Different Solvents and Linear Correlation Parameters[a] with E^*_{MLCT}[b]

	ν_{max}(MLCT), cm^{-1}						
metal(s)	toluene (0.30)	THF (0.59)	acetone (0.82)	DMF (0.95)	A[a]	B[a]	r[a]
Cr–Cr	15380	16210	16800	17240	14533	2818	0.999
Mo–Mo	16260	17240	18020	18350	15302	3257	0.999
W–W	15630	16450	17100	17640	14691	3028	0.997
Cr–Mo	15750	16750	17390	17760	14864	3081	0.998
Cr–W	15460	16260	16950	17390	14515	2954	0.999
Mo–W	15880	16670	17540	17950	14633	3228	0.997
Cr	17390	18180	18870	19230	16525	2845	1.000
Mo	18690	19610	20410	20620	17796	3063	0.996
W	18180	19050	19800	20000	17338	2886	0.996

[a] Parameters for the equation $\nu_{max} = A + BE^*_{MLCT}$ and the correlation coefficient r. [b] Solvent parameter taken from ref 21, given in parentheses after the solvent.

Table IV. ^{13}C NMR Spectra of dpp and $[M(CO)_4]dpp[M(CO)_4]$ Complexes

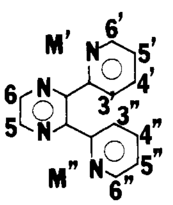

	$\delta(^{13}C)$[a]				
metal M′–M″	C(6), C(5)	C(6′), C(6″)	C(5′), C(5″)	C(4′), C(4″)	C(3′), C(3″)
dpp	148.38	142.46	122.78	136.16	123.87
Cr–Cr	154.21	144.12	126.58	136.21	127.42
Mo–Mo	153.40	143.96	126.79	136.52	127.94
W–W	153.69	144.68	128.05	136.63	128.66
Cr–W	154.16, 153.61	142.56, 144.61	b	136.20, 136.60	128.00, 128.57
W–Mo	153.76, 153.54	144.29	127.93, 127.19	136.83, 136.51	128.52, 128.30

[a] Chemical shift in CH_2Cl_2 reported vs Me_4Si.[1] [b] Only one distinct signal observed at 126.74 ppm.

The solvent sensitivity ($B = \nu_{max}/E^*_{MLCT}$) of the MLCT transition energy for the $[M(CO)_4]dpp$ and $[M(CO)_4]_2dpp$ complexes decreases slightly in the order M = Mo > W > Cr. The *B* value for $[Mo(CO)_4]dpp$ of 3058 is an intermediate value between the extremes for $[Mo(CO)_4]bpm$ (*B* = 4100, bpm = 4,4′-bipyrimidine) and $[Mo(CO)_4]abpy$ (*B* = 560, abpy = azo-2,2′-bis(pyridine)).[18,20] On the basis of comparative *B* values with other $[Mo(CO)_4]L$ complexes, this result suggests ddp is less effective at π back-donation than L = bpy, bpm, bpym, 2,2′-bipyrazine (bpz), or 3,3′-bipyridazine (bpdz).[18-20] The *B* value for $[Mo(CO)_4]_2dpp$ of 3256 also falls between extremes ($[Mo(CO)_4]_2bpym$, *B* = 4110; $[Mo(CO)_4]_2abpy$, *B* = 1460) and most closely approximates the value of 3110 reported for the isomeric 2,5-bis(2-pyridyl)pyrazine (dppz) ligand complex $[Mo(CO)_4]_2dppz$.[18-20] These results are consistent with previous solvatochromic studies which suggested that metal centers bound to stronger bases such as pyrimidines and pyrazines (greater σ donation) are more polarizable in the ground state than metal centers bound to weaker bases. The *B* values of the bimetallic dpp complexes (except Cr–Cr) are larger than those of the respective monometallic dpp complexes, consistent with two polarizable metal centers.[18] The *B* value decreases for heterobimetallic complexes in the order Mo–W > Mo–Cr > W–Cr as could be predicted from *B* values of the monometallic complexes.

The energy of the MLCT absorption in a given solvent decreased in the order M = Mo > W > Cr for $[M(CO)_4]dpp$ complexes and Mo–Mo > Mo–W > Mo–Cr > W–W > W–Cr ≥ Cr–Cr for $[M(CO)_4]dpp[M'(CO)_4]$ complexes. The decreasing energy trend for the monometallic series is consistent with that for other complexes of group 6 metal carbonyls.[20,21]

^{13}C NMR spectra for dpp and bimetallic dpp-bridged complexes were recorded in deuteriated dichloromethane (Table IV). The assignment of dpp signals is based on those for bpy and bpym.[16,22] Assignment of signals for homobimetallic complexes is based on dpp, and heterobimetallic signals are interpreted from the relative amount of shift from each metal in the homobimetallic complex. All ^{13}C signals in the bimetallic complexes shifted downfield (vs dpp), indicating stronger σ-donating effects predominate vs π-back-bonding contributions. The relative order of downfield shift for a carbon in homobimetallic complexes (M = Cr > W > Mo) parallels previous results for bpym complexes.[16,22]

Acknowledgment. We gratefully acknowledge the generous financial support of this work from the Research Corp.

Registry No. $[Cr(CO)_4]_2dpp$, 111468-79-2; $[W(CO)_4]_2dpp$, 111468-80-5; $[Mo(CO)_4]dpp[W(CO)_4]$, 111468-81-6; $[Mo(CO)_4]dpp[Cr(CO)_4]$, 111468-82-7; $[W(CO)_4]dpp[Cr(CO)_4]$, 111468-83-8; $[Cr(CO)_4]dpp$, 111468-84-9; $[Mo(CO)_4]_2dpp$, 105969-43-5; $[Mo(CO)_4]dpp$, 105969-42-4; $[W(CO)_4]dpp$, 111489-99-7; $W(CO)_6$, 14040-11-0; $Cr(CO)_6$, 13007-92-6; $Mo(CO)_6$, 13939-06-5.

Contribution from the Department of Chemistry,
Faculty of Science and Engineering,
Saga University, Honjo-machi, Saga, 840 Japan,
and Laboratory of Analytical Chemistry,
Faculty of Science, Nagoya University,
Chikusa-ku, Nagoya, 464 Japan

Importance of Hydrophobic Interaction in Metalloporphyrin Formation

Masaaki Tabata[1a] and Motoharu Tanaka*[1b]

Received July 30, 1987

Kinetic studies of metalloporphyrin formation may be helpful to understand the in vivo metal incorporation processes leading to the heme and chlorophylls.[2,3] The last step of the heme biosynthesis is the incorporation of iron(II) into protoporphyrin IX. The reaction does not occur readily and requires the enzyme of ferrochelatase.[4-6] Large metal ions such as mercury(II), cadmium(II), or lead(II) have been found to catalyze the metalloporphyrin formation.[7,8]

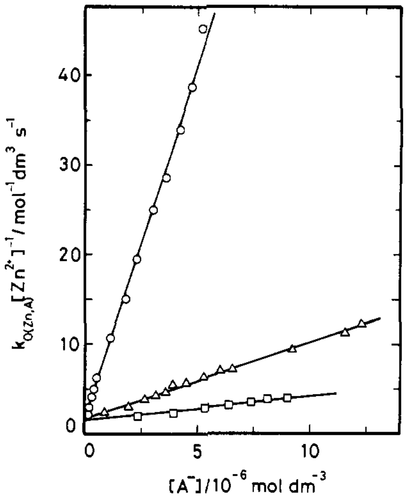

Figure 1. Plots of $k_{0(Zn,A)}[Zn^{2+}]^{-1}/mol^{-1}\,dm^3\,s^{-1}$ vs $[A^-]/10^{-6}\,mol\,dm^{-3}$ for L-tryptophan (○), L-phenylalanine (△), and glycine (□), where A^- denotes the anionic form of amino acid.

The present paper describes a catalytic effect of amino acids on the rate of metalloporphyrin formation. The reaction of zinc(II) with 5,10,15,20-tetrakis(4-sulfonatophenyl)porphine (H_2TPPS_4; charges on porphyrin and metalloporphyrin are omitted throughout) was found to be accelerated by amino acids (HA: glycine (Gly), L-α-alanine (Ala), L-valine (Val), L-phenylalanine (Phe), L-tyrosine (Tyr), and L-tryptophan (Trp), where HA denotes neutral form of amino acid). The catalytic effect of amino acids is discussed in terms of hydrophobic interaction of the amino acid side chain with porphyrin. The enhanced rate constant in the presence of amino acids is correlated with the hydrophobicity scale of amino acid residue.[9]

Kinetic studies were carried out in the pH range 6.0–7.0 (*N,N'*-bis(2-sulfonatoethyl)piperazine (PIPES) buffer, 5.0×10^{-3} mol dm^{-3}), at various concentrations of amino acid (1×10^{-5} to 4×10^{-2} mol dm^{-3}) and of zinc(II) (1×10^{-4} to 2×10^{-3} mol dm^{-3}) at 25 °C and $I = 0.1$ mol dm^{-3} ($NaNO_3$). The reaction was started by mixing a solution containing zinc(II) and amino acid with an H_2TPPS_4 solution (1.05×10^{-6} mol dm^{-3}). The change in absorbance at 421 nm (Soret band of $Zn^{II}(TPSS_4)$) was monitored as a function of time. The conditional formation rate constant of $Zn^{II}(TPPS_4)$, k_0, involving concentrations of hydrogen, zinc(II), and amino acid was determined from the first-order

---

[1] (a) Saga University. (b) Nagoya University.

[2] Tanaka, M. *Pure Appl. Chem.* **1983**, *55*, 151–158, and references therein.

[3] Lavallee, D. K. *Coord. Chem. Rev.* **1985**, *61*, 55–96, and references therein.

[4] Jones, M. S.; Jones, O. T. G. *Biochem. J.* **1970**, *119*, 453–462.

[5] Dailey, H. A., Jr.; Lascelles, J. *Arch. Biochem. Biophys.* **1974**, *160*, 523–529.

[6] Camadro, J. M.; Labbe, P. *Biochim. Biophys. Acta* **1982**, *707*, 280–288.

[7] (a) Tabata, M.; Tanaka, M. *Inorg. Chim. Acta Lett.* **1980**, *40*, X71. (b) Tabata, M.; Tanaka, M. *Anal. Lett.* **1980**, *13*(A6), 427–438. (c) Tabata, M.; Tanaka, M. *Mikrochim. Acta* **1982**, 149–158. (d) Tabata, M.; Tanaka, M. *J. Chem. Soc., Dalton Trans.* **1983**, 1955–1959. (e) Tabata, M. *Analyst (London)* **1987**, *112*, 141–144.

[8] Haye, S. E.; Hambright, P. *Inorg. Chem.* **1984**, *23*, 4777–4779.

[9] Nozaki, Y.; Tanford, C. *J. Biol. Chem.* **1971**, 246, 2211–2217. The hydrophobicity scale was experimentally determined by free energy of transfer of amino acids from water to organic solvent, and the value was recently used to analyze amino acid residues in globular proteins: Rose, G. D.; Geselowitz A. R.; Lesser, G. J.; Lee, R. H.; Zehfus, M. H. *Science (Washington, D.C.)* **1985**, *229*, 834–838.

* To whom correspondence should be addressed.

0020-1669/88/1327-0203$01.50/0 © 1988 American Chemical Society